

Technical Notes

TECHNICAL NOTES are short manuscripts describing new developments or important results of a preliminary nature. These Notes cannot exceed 6 manuscript pages and 3 figures; a page of text may be substituted for a figure and vice versa. After informal review by the editors, they may be published within a few months of the date of receipt. Style requirements are the same as for regular contributions (see inside back cover).

J80-157 Measurement of Shock Waves ²⁰⁰¹⁵ around a Delta-Wing Semicone ²⁰⁰¹⁷

Takeyoshi Kimura* and Masatomi Nishio†
Kobe University, Nada, Kobe, Japan

freestream density = 4×10^{-4} kg·s²/m⁴, duration time = 10 ms, and exit diameter of the nozzle = 15 cm.

Figure 1 shows a sketch of the delta-wing semicone model. The vertex angles of the delta-wing and the semicone body are 60 and 30 deg, respectively, which are made of Bakelite and plastic. Ten positive electrodes were located in the model and negative electrodes of the same number were installed in the freestream as shown in the figure.

Introduction

OBSERVATIONS of shock waves around hypersonic vehicles have been carried out by optical systems such as schlieren methods, Mach-Zehnder interferometers, and shadowgraphs. However, these methods are not suitable to measure the shock shapes of a wing body because it is difficult to observe the shock pattern between a wing and a body. For this reason, several techniques to visualize cross-sectional shock shapes have been developed recently. The electron beam method,¹⁻⁴ the vapor screen method,^{5,6} and the electric discharge method⁷ are useful for this purpose.

The electric discharge method was recently reported by Kimura, et al.⁷ Its principle is as follows: when an electric discharge is generated across a shock wave, the radiation intensity in a shock layer differs from the freestream according to the density difference. The location of the shock wave is easily observed by taking a photograph of the discharge column.

In this paper, we used the electric discharge method to visualize the cross-sectional shock shapes around a delta-wing semicone body. The primary purposes are to determine the variations of shock patterns with angle of attack and to visualize the cross-sectional shock shapes.

Experiments and Discussion

A hypersonic gun tunnel was used in this experiment. The characteristics of the hypersonic gun tunnel is as follows: Mach number = 10, Reynolds number = 2×10^4 cm⁻¹, freestream velocity = 10^3 m/s, static pressure = 0.4 Torr,

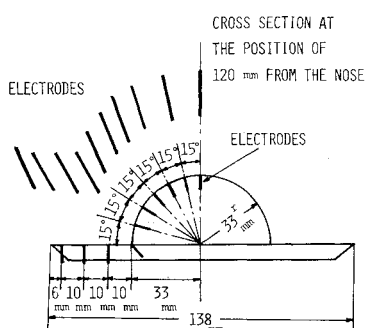


Fig. 1 Delta-wing semicone model.

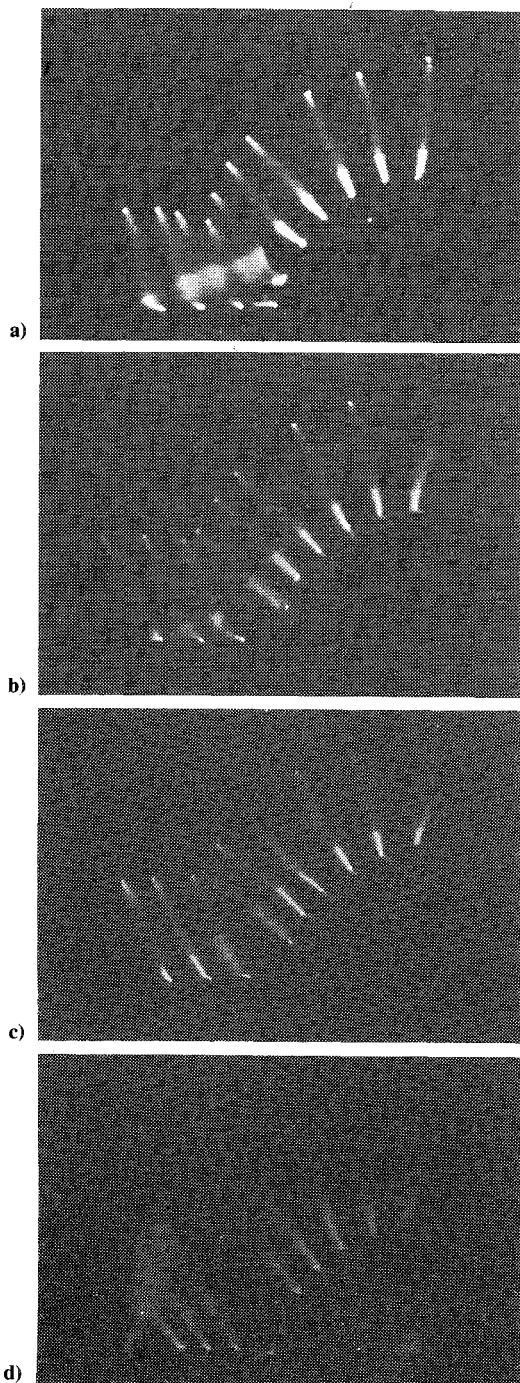


Fig. 2 Experimental results of shock shapes: a) $\alpha = 0$ deg, b) $\alpha = 10$ deg, c) $\alpha = 20$ deg, and d) $\alpha = 30$ deg.

Received April 14, 1979; revision received Nov. 9, 1979. Copyright © American Institute of Aeronautics and Astronautics, Inc., 1979. All rights reserved.

Index categories: Shock Waves and Detonations; Supersonic and Hypersonic Flow.

*Professor, Dept. of Mechanical Engineering. Member AIAA.

†Research Associate, Dept. of Production Engineering. Member AIAA.

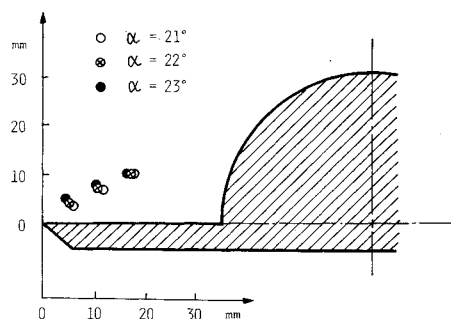


Fig. 3 Experiments of leading edge.

The radius of the blunted nose was less than about 0.05 cm in diameter, that is, Reynolds number was about 10^5 . The measurements were carried out at the position of 120 mm from the nose, as shown in Fig. 1. According to Chernyi,⁸ a flow pattern around a slightly blunted cone becomes almost the same as a pointed cone, in the case that bluntness factor $\sqrt{2}/C_D \cdot x/d \cdot \tan^2 \beta$ is larger than about 1.5, where C_D , x , d , and β are the drag coefficient, distance from the nose, radius of the blunted nose, and semiapex angle of the nose, respectively. If the theory can be applied to our case, the flow pattern in this experiment may be considered to be a conical flow since the bluntness factor is about 70.

Figure 2 showed the experimental results for the angles of attack $\alpha = 0, 10, 20$, and 30 deg. Double shock patterns, which consisted of a wing shock and a body shock, occurred in cases of $\alpha = 0$ and 10 deg. On the other hand, single shock patterns, compounded by a wing shock and a body shock, appeared in cases of $\alpha = 20$ and 30 deg. The results of the double shock patterns agreed well with those obtained by the vapor screen method.⁶

More precise experiments near the wing leading edge were carried out in cases of $\alpha = 21, 22$, and 23 deg, and the results were shown in Fig. 3. At $\alpha = 21$ deg, the shock wave was attached at the leading edge, while it was detached from the leading edge at $\alpha = 22$ and 23 deg. This agreed approximately with the result of Ref. 9.

At $\alpha = 0$ or 10 deg, it was impossible to observe the corner shock wave by an optical system, since light paths were prevented from passing through by the wing or the body. The electric discharge method is superior to any optical method in this respect.

References

- 1 Weinstein, L. M., Wagner, R. D., Jr., and Ocheltree, S. L., "Electron Beam Flow Visualization in Hypersonic Helium Flow," *AIAA Journal*, Vol. 6, Aug. 1968, pp. 1023-1025.
- 2 Muntzs, E. P. and Marsden, D. J., *Investigation of Flows with Electron Beam*, pp. 495-526.
- 3 Rothe, D. E., "Flow Visualization Using a Traversing Electron Beam," *AIAA Journal*, Vol. 3, Oct. 1965, pp. 1945-1946.
- 4 Maguire, B. L., Mallin, J. R., and Muntzs, E. P., "Visualization Technique for Low-Density Flow Fields," *IEEE Transactions*, Vol. AES-3, No. 2, 1967, pp. 321-326.
- 5 Rao, D. M., "Delta Wing Shock Shape at Hypersonic Speed," *AIAA Journal*, Vol. 9, Oct. 1971, pp. 2093-2094.
- 6 Scheuing, R. A., "Outer Inviscid Hypersonic Flow with Attached Shock Waves," *ARS Journal*, April 1961, pp. 486-505.
- 7 Kimura, T., Nishio, M., Fujita, T., and Maeno, "Visualization of Shock Wave by Electric Discharge," *AIAA Journal*, Vol. 15, May 1977, pp. 611-612.
- 8 Chernyi, G. G., *Introduction to Hypersonic Flow*, Academic Press, New York, 1961, pp. 226-231.
- 9 Goebel, T. P., Martin, J. J., and Boyd, J. A., "Factors Affecting Lift-Drag Ratios at Mach Numbers from 5 to 20," *AIAA Journal*, Vol. 1, March 1963, pp. 640-650.

J80-158

Analysis of the Strong Interaction Problem with Slip and Temperature-Jump Effects

20013

20017

R. N. Gupta* and S. Menon†

Indian Institute of Technology, Kanpur, India
and

C. M. Rodkiewicz‡

University of Alberta, Edmonton, Canada

Introduction

THE analysis of the hypersonic interaction problem without slip and temperature-jump conditions on a flat plate by utilizing the boundary-layer equations is well documented.^{1,2} For the interaction problem with slip and temperature-jump effects, Ref. 3 has provided a solution which is an expansion in terms of the slip parameter about the no-slip strong interaction solution. Analysis of Ref. 3, however, would be more appropriate for the cold wall case where the slip and temperature-jump effects are much smaller. The momentum integral-equation formulation of Ref. 4 suffers from the fact that the use of a linear velocity profile does not allow a complete accounting of the viscous effects in the momentum equation. Further, in this approach the integrator is started right from $x=0$, thus covering the noncontinuum flow and continuum-merged flow regimes where the boundary layer equations cannot, strictly speaking, be used. In the present analysis, a finite-difference solution to the strong interaction problem with slip and temperature-jump effects is given by utilizing the boundary layer equations.

Flow Equations and Discussion of Results

Under the assumption of a linear viscosity relation of the form $\mu = CT$, the transformed boundary-layer momentum and energy equations may be written in terms of the dimensionless stream function f and the dimensionless total enthalpy H as²

$$\begin{aligned} \bar{p} \frac{\partial^3 f}{\partial \eta^3} + f \frac{\partial^2 f}{\partial \eta^2} - 4x \left(\frac{\partial f}{\partial \eta} \frac{\partial^2 f}{\partial x \partial \eta} - \frac{\partial f}{\partial x} \frac{\partial^2 f}{\partial \eta^2} \right) \\ = \left(\frac{\gamma-1}{\gamma} \right) \left(\frac{2x}{\bar{p}} \frac{d\bar{p}}{dx} - 1 \right) \left[H - \left(\frac{\partial f}{\partial \eta} \right)^2 \right] \end{aligned} \quad (1)$$

$$\begin{aligned} \frac{\bar{p}}{Pr} \frac{\partial^2 H}{\partial \eta^2} + f \frac{\partial H}{\partial \eta} - 4x \left(\frac{\partial f}{\partial \eta} \frac{\partial H}{\partial x} - \frac{\partial f}{\partial x} \frac{\partial H}{\partial \eta} \right) \\ = \frac{2(1-Pr)}{Pr} \bar{p} \left[\left(\frac{\partial^2 f}{\partial \eta^2} \right)^2 + \frac{\partial f}{\partial \eta} \frac{\partial^3 f}{\partial \eta^3} \right] \end{aligned} \quad (2)$$

In order to bring out the character of strong interaction solutions as distinct from weak interactions, pressure has been retained as a coefficient of higher order terms in Eqs. (1) and

Received June 20, 1979; revision received Nov. 15, 1979. Copyright © American Institute of Aeronautics and Astronautics, Inc., 1979. All rights reserved.

Index categories: Rarefied Flows; Supersonic and Hypersonic Flow.

*Professor, Dept. of Aeronautical Engineering. Member AIAA.

†Presently, Dept. of Aerospace Engineering, University of Maryland.

‡Professor of Mechanical Engineering.

In fond memory of M. H. Bertram with whom one of us (RNG) spent many fruitful years.